THE ASTROPHYSICAL JOURNAL, 230:782–785, 1979 June 15

DISCOVERY OF TWO DISTORTED INTERSTELLAR BUBBLES

T. R. GULL* and S. SOFIA†
Laboratory for Astronomy and Solar Physics,
Goddard Space Flight Center
Received 1978 October 30; accepted 1978 December 19

ABSTRACT

During an extensive program of direct imagery of emission nebulae, arcuate structures have been found around two stars. A well-defined shocklike structure is found about the T Orionis variable LL Ori, located to the side of the Orion Nebula. A less extensive shocklike structure is also found about the runaway star ζ Oph. These structures can be best described in terms of distorted interstellar bubbles. A direct consequence of this interpretation is an independent estimate of the rates of mass loss for these stars.

Subject heading: nebulae: general

I. INTRODUCTION

During the past 5 years one of the authors, T. Gull, has been carrying out an extensive study of galactic emission nebulae by using direct imagery through narrow-passband interference filters. Bright emission lines characteristically emitted by a variety of emission nebulae, and selected regions of the continuum, are well isolated by the filters used in this study. Selected bright H II regions were observed by using the prime focus cameras of both the KPNO and Cerro Tololo 4 m telescopes. Passbands isolating Hα + [N II], [S II], [O III], and continuum were used to record the brightest portions of these nebulae with a few arcseconds resolution. A complete, sky-background–limited survey in light of Hα + [N II], [S II], [O III], Hβ, and continuum has been made encompassing the galactic zone between the latitudes +7° and −7° and emission nebulae of special interest located beyond this zone. This is being published shortly as a NASA special publication by Parker, Gull, and Kirshner (1979). From a preliminary examination of all of this material, we noted two unusual, well-defined arcuate structures centered upon remarkably dissimilar stars. In § II, we shall gather all of the observational material relating to these objects. We give an interpretation of their physical nature in § III, and § IV contains a discussion regarding what can be learned from these distorted interstellar bubbles.

II. OBSERVATIONS

a) Direct Imagery

Direct imagery through interference filters is proving to reveal many new and intriguing emission-line structures, both of new emission nebulae and within known, classical nebulae. For example, the galactic plane survey has detected several new emission nebulae, most notably a 3° × 4° supernova remnant in Cygnus (Gull, Kirshner, and Parker 1977). The doubly ionized oxygen in the Orion Nebula is diffuse and concentrated near θ^1 Ori, while the singly ionized sulfur structure is defining the ionization boundary near the dark cloud (Gull, 1974). Rejection of the diffuse continuum and hydrogen emission reveals hitherto unexpected substructures accentuated by the forbidden-line emission. These substructures include Herbig-Haro objects, ionization-bound zones, and an arcuate structure.

The arcuate structure about LL Ori has been recorded in countless photographs. However, it has only recently been noted as a consequence of the present study. In Figure 1 (Plate 14) we present the Hβ image of the Orion Nebula which best reveals the characteristics of the structure around LL Ori. Reproduction of the entire structure as seen on the original plates is most difficult because of the rapidly changing nebular background. The figure indeed shows the most salient aspects—namely, the arcuate structure is symmetrical about an axis pointing toward the brighter portion of the Orion Nebula, and is roughly parabolic in shape. It is discernible that the arcuate structure is displaced slightly (about 3″) from the stellar image of LL Ori. Moreover, there is a wake following the star. Examination of the original plate shows that the arcuate structure can be traced up to 5′ away from the head of the arc. It becomes progressively more diffuse until the contrast becomes too low to be visible. The most obvious characteristics of this structure are shown in Figure 2 (Plate 15).

The arcuate structure, while most visible in Hβ, is also easily seen in light of [S II] (6717 Å), [O II] (3727 Å), and [N II] (6584 Å). The structure is visible in [O III] (5007 Å), He I (5875 Å), and Hα (6563 Å), but is noticeably more diffuse and has much less contrast because of the very bright nebular background. In fact, the head of the arc, that portion closest to the star,

* Visiting Astronomer at Kitt Peak National Observatory and Cerro Tololo Inter-American Observatory, which are sponsored by the Association of Universities for Research in Astronomy, Inc., under contract with the National Science Foundation.

† NAS/NRC Senior Research Associate.

can be noted in a red continuum, 90 Å wide passband centered at 6470 Å.

Independent confirmation of the arcuate structure was recorded by using narrower passband interference filters with an image intensifier on the KPNO No. 1 92 cm telescope. Perhaps the most widely distributed example of the structure is the Lick three-color photograph which has appeared as the front cover on both *Scientific American* (1974 October) and *Physics Today* (1973 March).

The arcuate structure noticed about ζ Oph has been seen most readily in the light of [O III] (Fig. 3 [Pl. 16]). However, it is faintly visible in the light of Hα + [N II]. The images were recorded by using the galactic plane survey instrument, which is a Nikkor ED 300 mm f/2.8 camera lens and two-stage image intensifier. Details of the instrument are being published with the survey (Parker, Gull, and Kirshner 1979). This instrument achieves sky-background–limited [O III] images through a 28 Å wide filter in 20 minutes. However, the angular resolution is about ½′ over a 7° field of view.

It would seem astonishing that the 3/4° long structure in [O III] (about 3 pc at the distance of ζ Oph) has not been noted before despite numerous observations of the ζ Oph region. However, the Palomar Sky Survey does not record the structure because the photographic emulsion used for the blue survey only weakly responds to 5000 Å, while passing a large portion of the blue continuum. The nebulosity is so faint in [O III] that only a narrow filter passband is sufficient to reject the diffuse continuum, and a very fast optical system is needed to record the low surface brightness. The sensitivity of the image-intensified 300 mm survey instrument is perhaps fully appreciated by noting that the equivalent 4 m prime focus exposure is estimated to be 24 hours!

The structure about ζ Oph is also symmetrical, but much less curved compared with the LL Ori structure. The leading edge is separated from the stellar image by about 5′. Upper limits to the [S II] and blue (4215 Å) continuum structure are 3 times fainter than the detected [O III] structure. The Hα + [N II] structure is at least 2 times fainter than the [O III] structure.

b) *Spectroscopy*

At present, spectroscopic information exists only for the LL Ori structure. Measures of the [S II] (6717 Å, 6731 Å) doublet ratio and the [O III] (3726 Å, 3729 Å) doublet ratio indicate the nebular density in the vicinity of the arc head to be about 10^3 cm^{-3}. With angular resolution of several arcseconds, there is no strong emission detected from the arc. This is due to the low surface brightness of the arc compared with the background nebula, and also because the thickness of the arc is below an arcsecond; hence, the structure is smeared out by spectroscopic observations even with the Cassegrain spectrograph on the KPNO 4 m telescope. Moreover, no high-velocity structure along the line of sight is noted in echellograms recorded using the Cassegrain echelle spectrograph on the KPNO 4 m telescope. This is very different from two other classes of shocked phenomena, namely, Herbig-Haro objects and structure near θ^2 Ori also present in the Orion Nebula.

Spectra of LL Ori were recorded in the red using the Kitt Peak 4 m echelle spectrograph at 6 Å mm^{-1} and the 4 m Cassegrain spectrograph at 25 Å mm^{-1}. These spectra show that Hα is in broad, complex emission signifying mass loss. Furthermore, the Hα profile was found to change within a 3 day interval. Structure of the line is noticeable from -400 km s^{-1} to $+600$ km s^{-1}. Hence the terminal velocity of this star is at least 600 km s^{-1}.

c) *Other Related Observations*

The star LL Ori has been classified (Parenago 1954) to be a T Orionis variable with a KO:e spectral class. ζ Oph is an O9.5 V star (Lesh 1968). LL Ori has a proper motion $\mu = 0\farcs0033$ year^{-1} (Fallon 1979) which at 500 pc corresponds to a $v_T \approx 8$ km s^{-1}. The published radial velocity of LL Ori is $+17$ km s^{-1} with a very large probable error of the order of 7.4 km s^{-1} (Johnson 1965). These values lead to a space velocity of 19 km s^{-1}. ζ Oph is a well-known runaway star (Blaauw 1961), and it is an FK4 catalog star. The value of μ is $0\farcs0252$ year^{-1} which at 180 pc distance corresponds to $v_T = 21.5$ km s^{-1}. The radial velocity (Blaauw 1961; Morton 1976) is -19 km s^{-1} with an accuracy presumably similar to that of the LL Ori measured velocity. This results in a space velocity of 29 km s^{-1}.

Zeta Oph is a mass-losing star with a terminal velocity of 1350 km s^{-1} as measured by *Copernicus* (Morton 1976; Snow and Morton 1976). Determinations of the mass-loss rate do not exist for this star. However, a good estimate for that quantity can be made by applying a scaling law derived by Cassinelli (1978), based upon the results of Abbott (1978). Cassinelli found that $\dot{m} \propto L^{1.3}$ where L is the stellar luminosity. We can now compare our star with τ Sco, which has been modeled in detail by Lamers and Rogerson (1978), who obtained $\dot{m} = 7 \times 10^{-9}\ M_\odot$ year^{-1}. Since ζ Oph is 1.1 mag brighter than τ Sco, the scaling leads to a mass-loss rate of $2.2 \times 10^{-8}\ M_\odot$ year^{-1} for ζ Oph.

A concluding statement regarding ζ Oph can be made on the emission nebula surrounding the star. Radio observations, Hα surface brightness measures, and studies of the interstellar absorption lines (see as reviewed by Herbig 1968 and Morton 1976) lead to an electron-density estimate within the H II region of $N_e \approx 3$ cm^{-3}.

III. INTERPRETATION

a) *Similarities and Differences*

The most obvious similarities of these two structures are that both stars are losing mass and are surrounded by emission nebulae. It is surprising, though, to note that the spectral types are very different. The sound speed for an H II region, which has approximately

solar composition and an electron temperature of 10^4 K, is 12 km s^{-1}. The space motions of ζ Oph and LL Ori are clearly supersonic, and the existence of shock phenomena must be implied.

The velocity which plays the critical role in shock phenomena is the velocity relative to the immediately surrounding medium rather than the space velocity. It is known from independent sources (Balick, Gull, and Smith 1979) that the ionized gas in the vicinity of LL Ori is moving away from the dark cloud at about the sound speed. That is interpreted to mean that the ultraviolet radiation from the exciting stars, θ^1 Ori, penetrates into the dark cloud, ionizing it layer by layer, and causing the ionized gas to expand toward the more rarefied surrounding space. It is particularly significant to note that the arcuate structure points not at θ^1 Ori, but at the ionizing boundary known as the Bar (indicated in Fig. 1). We note that, since the proper motion of LL Ori is directed toward θ^1 Ori (Fallon 1979), the dominant component of the relevant tangential velocity is that of the gas. An approximate value for this relative velocity is 20 km s^{-1}.

We have no corresponding evidence for systematic mass motion for the H II region surrounding ζ Oph; we shall henceforth assume that no such components exist. In this case, the net velocity direction is about 44° with respect to the plane of the sky. The projected velocity direction in the plane is about 20° east of north and is indicated in Figure 3. It is noteworthy that the projected axis of symmetry of the arc is in the general direction of motion.

b) *Modeling of the Structures*

The structures are produced by the interaction of a strong stellar wind with supersonic streaming interstellar gas. A situation of this nature has been modeled by Castor, McCray, and Weaver (1976) and by Weaver *et al.* (1977), and it corresponds to what they described as a *distorted interstellar bubble*. We can first use this interpretation to compute the rate of mass loss from the stars. At the head of the arc, we are dealing with a simple shock, and at the boundary the stellar wind pressure approximately equals the ram pressure of the interstellar material:

$$\frac{\dot{m}}{4\pi r^2_{\rm min}} \times v_T = \rho v^2 , \qquad (1)$$

where $\dot{m}$ is the rate of mass loss in cgs units, v_T is the terminal velocity of the wind, $r_{\rm min}$ is the separation or distance from the star to the head of the bow arc, ρ is the total mass density of the undisturbed ionized gas, and v is the relative velocity of the star with respect to the surrounding gas. For the case of LL Ori ($v = 28$ km s^{-1}, $v_T = 600$ km s^{-1}, $\rho = 1.6 \times 10^{-21}$ g cm^{-3}, $r_{\rm min} = 2 \times 10^{16}$), the derived mass-loss rate is 9×10^{17} g s^{-1} or $1.5 \times 10^{-8}\ M_\odot$ per year. No independent mass-loss rate determination exists for LL Ori. For the case of ζ Oph ($v = 28$ km s^{-1}, $v_T = 1350$ km s^{-1} (Morton 1976; $\rho = 5 \times 10^{-24}$ g cm^{-3}, $r_{\rm min} = 7 \times 10^{17}$ cm), the derived mass-loss rate is 1.5×10^{18} g s^{-1} or $2.3 \times 10^{-8}\ M_\odot$ year^{-1}. This mass-loss rate for ζ Oph is in excellent agreement with the value of $2.2 \times 10^{-8}\ M_\odot$ year^{-1} obtained in § II of this paper.

The shape of the bow shock (Weaver, McCray, and Castor 1977) is a paraboloid of revolution whose axial cross section is given by

$$Y(z) = \left(\frac{20 L_w}{33\pi\rho v^3}\right)^{1/4} z^{1/2} , \qquad (2)$$

where L_w is the mechanical luminosity (or the kinetic energy loss rate)

$$L_w = \tfrac{1}{2}\dot{m} v_T^2 , \qquad (3)$$

z is the distance along the axis of symmetry from the shock head, and $Y(z)$ is the distance orthogonal to the axis of symmetry.

For the case of LL Ori, the shape we derived from equation (2) is more closed than the observed structure. The discrepancy can be understood in terms of either of two possibilities. First, there is a projection effect where the observed z displacement is the foreshortened true displacement:

$$z_{\rm observed} = z \cos i . \qquad (4)$$

This results in the parabolic surface effectively opening up by a factor of $(\cos i)^{-1}$, where i is the inclination of the symmetry axis with respect to the plane of the sky. The approximate values for the tangential and radial velocities lead to an inclination angle of 45°. However, this widening is not sufficient to bring the theoretical shape of the shock into coincidence with the observed structure. In order to do this we must use an inclination angle of 50°. This value is not inconsistent with the accuracy of the observations. Alternatively, we know that the electron density decreases from 2×10^3 cm^{-3} in the core of the nebula to 2×10^1 cm^{-3} 10′ away in the general direction past the LL Ori region (O'Dell and Hubbard 1964). Since ρ appears in the denominator of equation (2), a gradual decrease in electron density would also contribute to opening up the paraboloid. The actual situation is very likely a combination of both effects. However, in Figure 2 we show the 50° projected cone.

For ζ Oph the radial velocity and the tangential velocity lead to an inclination angle of 40°, hence, the paraboloid is foreshortened by a factor of 1.3. The resulting shape is displayed in Figure 4 (Plate 17) along with the observed shape. We feel that the agreement is very good.

IV. CONCLUSIONS AND DISCUSSION

It appears from the above section that the observations are adequately explained in terms of the distorted interstellar bubble theory, and thus we conclude that that is indeed what we have observed. From the smoothness of shape and extent of both structures, it would appear that discontinuous condensations are

not significant in these H II regions. A final conclusion is that these structures are extremely powerful tools to determine rates of mass loss from stars with quite different spectral types. The three requirements for the existence of these structures, namely, a star with a strong stellar wind moving supersonically with respect to a surrounding H II region, are not terribly restrictive, and hence there should be many of such objects in the Galaxy. The dearth of discovery can be accounted for by the nearly monochromatic emissions, the low surface brightness, extreme thinness of the structure, and superposition upon the nebular background. Keeping these limitations in mind, a well-directed search should greatly enlarge our sample and cover mass loss from stars at various stages of evolution.

We wish to acknowledge the helpful comments of an anonymous referee who gave us new insight on LL Ori.

REFERENCES

Abbot, D. C. 1978, *Ap. J.*, **225**, 893.
Balick, B., Gull, T. R., and Smith, M. G. 1979, in preparation.
Blaauw, A. 1961, *Bull. Astr. Inst. Netherlands*, **15**, 265.
Cassinelli, J. P. 1978, private communication.
Castor, J., McCray, R., and Weaver, R. 1975, *Ap. J.* (*Letters*), **200**, L107.
Fallon, F. 1979, in preparation.
Gull, T. R. 1974, in *8th ESLAB Symposium on* H II *Regions and the Galactic Center*, ed. A. F. M. Moorhead (ESRO SP-105), p. 1.
Gull, T. R., Kirshner, R. P., and Parker, R. A. R. 1977, *Ap. J.* (*Letters*) **215**, L69.
Herbig, G. 1968, *Zs. Ap.*, **68**, 243.
Johnson, H. M. 1965, *Ap. J.*, **142**, 964.
Lamers, H. J. G. L. M., and Rogerson, J. B. 1978, *Astr. Ap.*, in press.
Lesh, J. R. 1968, *Ap. J. Suppl.*, **17**, 371.
Morton, D. 1976, *Ap. J.*, **203**, 386.
O'Dell, C. R., and Hubbard, W. B., 1964, *Ap. J.*, **142**, 591.
Parenago, P. P. 1954, *Trudy Sternberg Astr. Inst.*, **25**.
Parker, R. A. R., Gull, T. R., and Kirshner, R. P. 1979, *An Emission Line Survey of the Milky Way*, NASA, in preparation.
Snow, T., and Morton, D. 1976, *Ap. J. Suppl.*, **32**, 429.
Weaver, R., McCray, R., and Castor, J. 1977, *Ap. J.*, **218**, 377.

T. R. Gull: Code 683, Laboratory for Astronomy and Solar Physics, Goddard Space Flight Center, Greenbelt, MD 20771

S. Sofia: Code 681, Laboratory for Astronomy and Solar Physics, Goddard Space Flight Center, Greenbelt, MD 20771

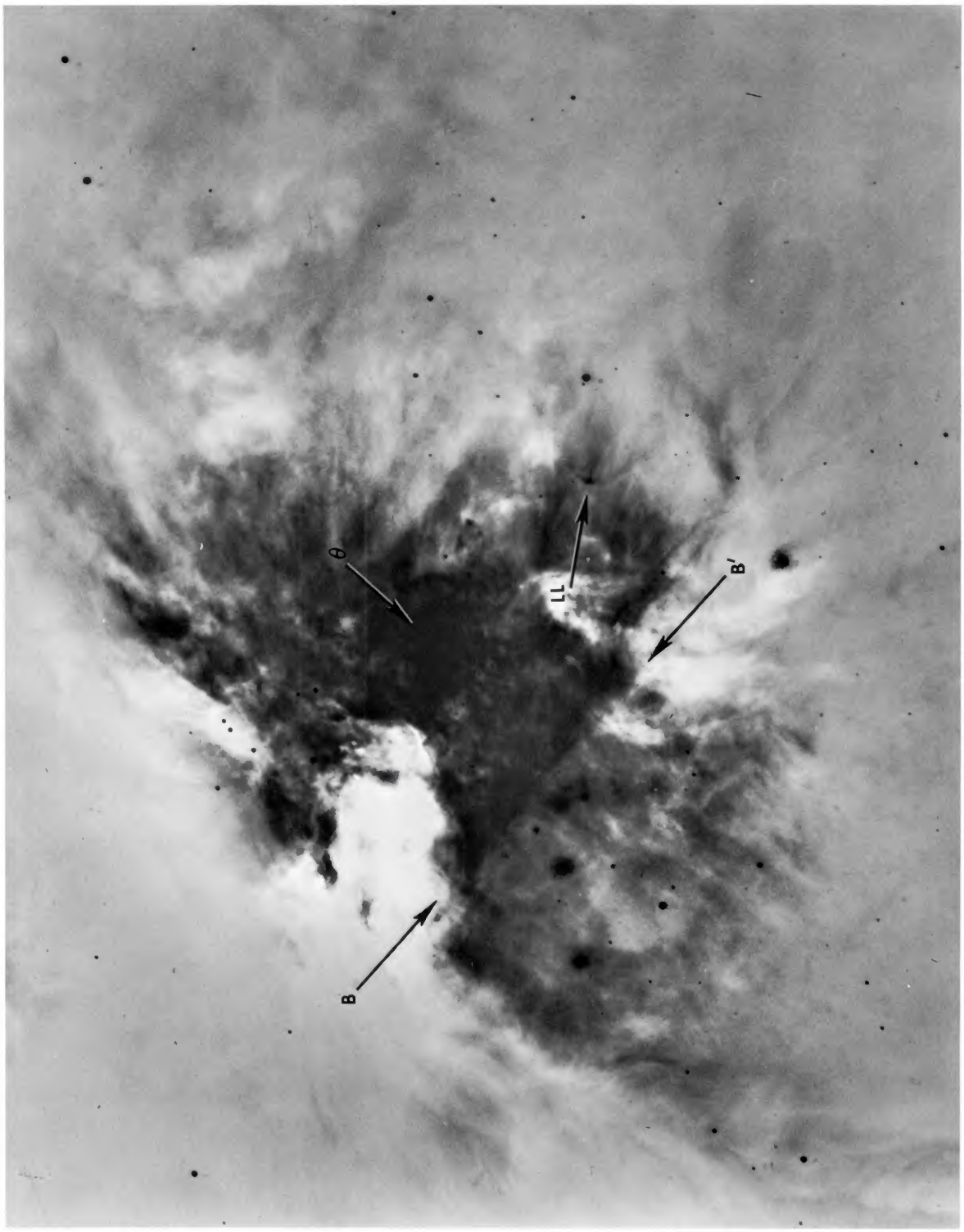

FIG. 1.—The Orion Nebula as recorded through a 60 Å wide Hβ interference filter on the KPNO 4 m prime focus camera. The arrow indicates LL Ori and the arcuate structure around it. The arrow labeled θ indicates the position of θ^1 Ori. Arrows labeled B and B′ define the Bar structure. Note that the axis of symmetry points toward the Bar structure, not θ^1 Ori.

PLATE 15

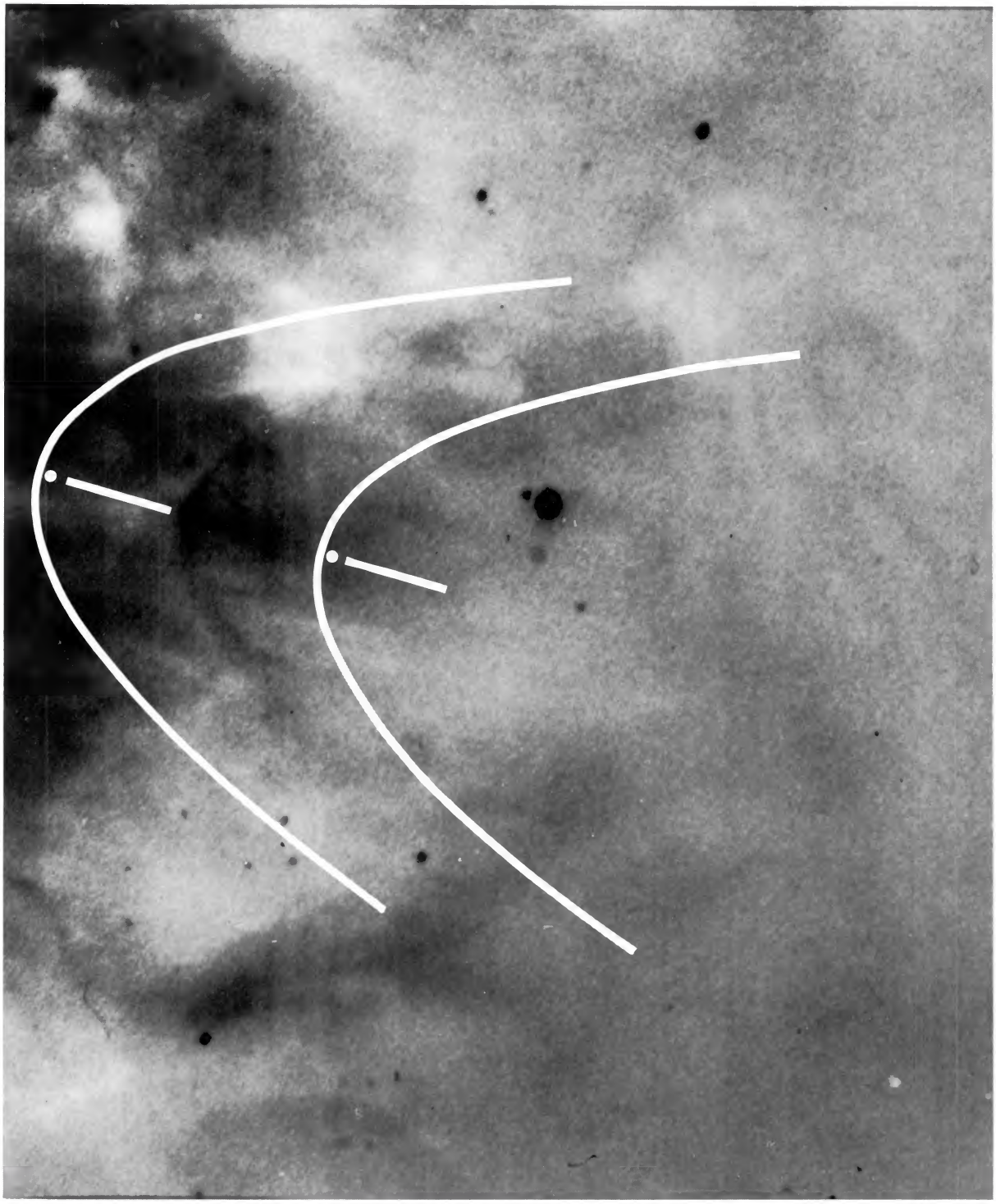

FIG. 2.—A blown-up view from Fig. 1 shows the arcuate structure in more detail. Displaced ahead of and behind the structure is the calculated shape (*see text*).

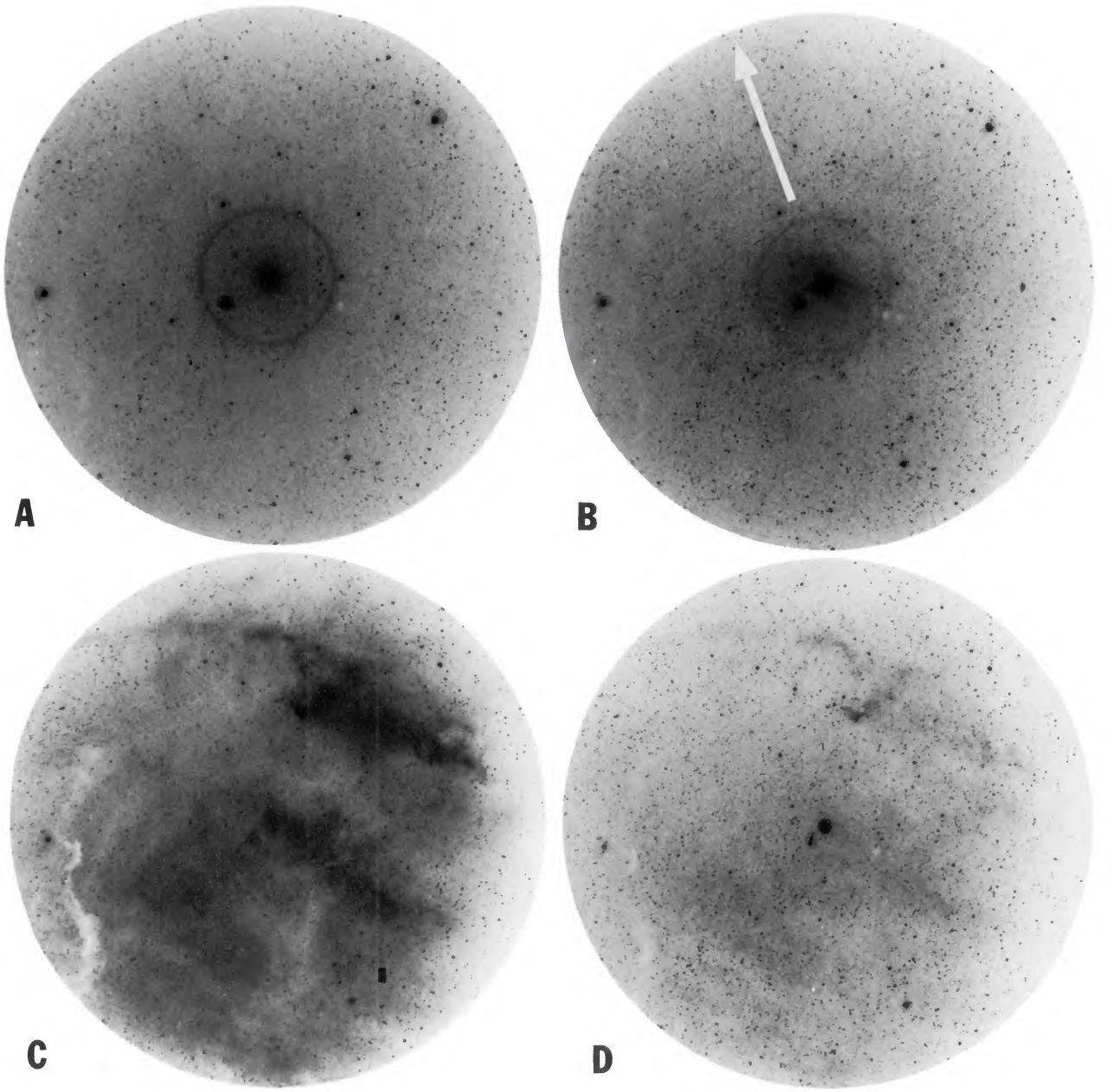

FIG. 3.—Four passbands of the ζ Oph H II region are shown here. Fig. 3*a* is through a blue continuum passband (4225 Å, $\Delta\lambda = 60$ Å), Fig. 3*b* is through an [O III] passband (5010 Å, $\Delta\lambda = 28$ Å), Fig. 3*c* is through an Hα + [N II] passband (6570 Å, $\Delta\lambda = 75$ Å), and Fig. 3*d* is through an [S II] passband (6736 Å, $\Delta\lambda = 50$ Å). The arcuate structure is most visible in [O III], and faintly visible in Hα + [N II]. It is not detected in [S II] or blue continuum. The large ring around the star image is a reflection due to the transfer lens located after the image intensifier, and the ghost that appears to the side of the star image (indicated in Fig. 3*a*) is due to opposite field reflection off the interference filter. As these plates were recorded, identical frames were recorded of α, δ, σ, π, and τ Sco with the star images in precisely the same position on the camera field. None of the plates show arcuate structures like that seen about ζ Oph in [O III]. Furthermore, a number of frames recorded with a 135 mm camera also detect the [O III] around ζ Oph. The arrow indicates the proper-motion direction of ζ Oph as published in the FK4 catalog.

GULL AND SOFIA (*see* page 783)

PLATE 17

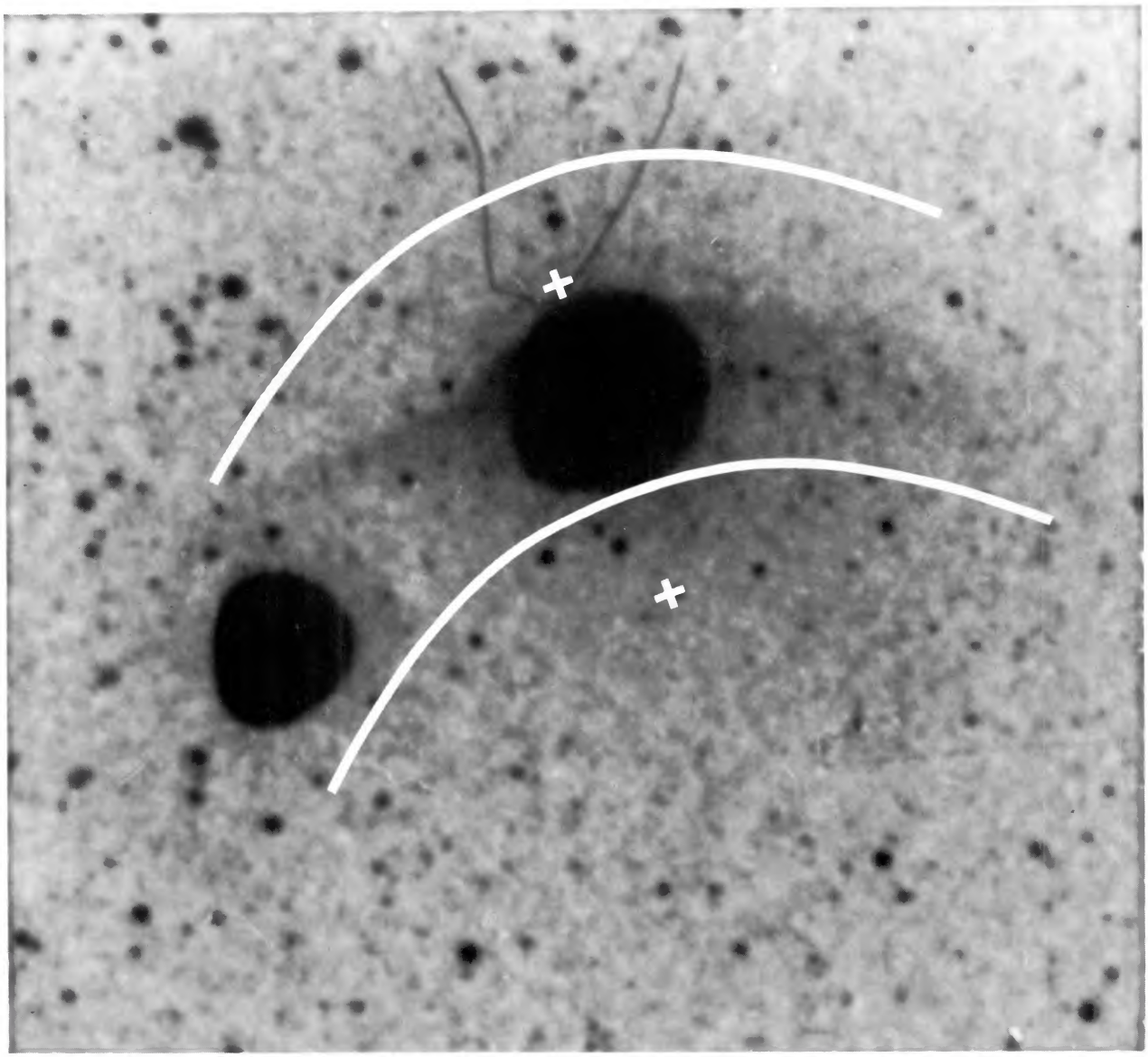

FIG. 4.—Expanded view of the [O III] arcuate structure around ζ Oph. Displaced ahead and behind the arc is the calculated shape of the shock.

GULL AND SOFIA (*see* page 784)